Energy, Mines and Resources Canada
Énergie, Mines et Ressources Canada

CANMET

Canada Centre for Mineral and Energy Technology
Centre canadien de la technologie des minéraux et de l'énergie

Mining Research Laboratories
Laboratoires de recherche minière

ELECTRICAL CHARGE CHARACTERISTICS OF LONG-LIVED RADIOACTIVE DUST

J. BIGU ELLIOT LAKE LABORATORY

MRL 89-71(J) MARCH 1990

Canada

MRL 89-71 (J) e.2

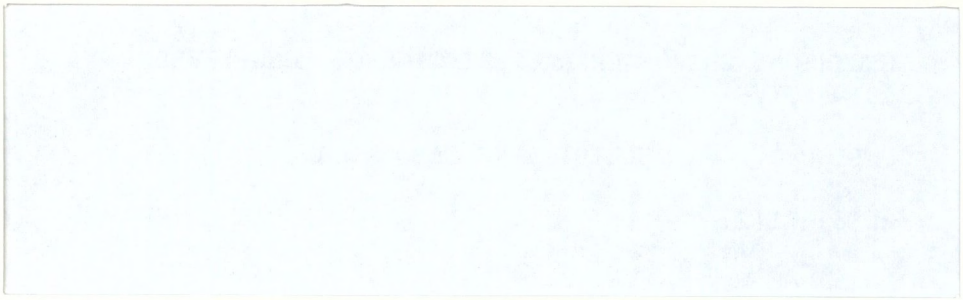

ELECTRICAL CHARGE CHARACTERISTICS OF LONG-LIVED RADIOACTIVE DUST

J. BIGU ELLIOT LAKE LABORATORY

MRL 89-71(J) MARCH 1990

Published in Health Physics, Volume 58, No. 3, pp 341 to 350, March 1990

ELECTRICAL CHARGE CHARACTERISTICS OF LONG-LIVED RADIOACTIVE DUST

J. Bigu*

ABSTRACT

Respirable long-lived radioactive dust (LLRD), i.e., dust containing long-lived radionuclides such as ^{238}U, ^{232}Th, ^{226}Ra, ^{224}Ra and ^{228}Th, interacts with unipolar and bipolar atmospheres through diffusion charging, electrical charge neutralization, and electrical self-charging mechanisms. Because of these interactions, and depending on the type of dust as well as its method of production, LLRD is found in electrically charged, and neutral states. Electrical charge is important because it influences the deposition of particles in the human respiratory system. Particle size, electrical charge, and radioactive particle size distributions were measured in an area of an underground U mine where U ore crushing and transportation operations were conducted. In addition, concurrent measurements of ^{222}Rn progeny and ^{220}Rn progeny were made. A variety of instrumentation was used, such as particle counters. The electrical charge associated with dust generated in the primary crushing operation was substantially higher (3 e^- at 1 μm and ~500 e^- at 3 μm) than for the conveyor belt (2 e^- at 1 μm and ~50 e^- at 8 μm). In both cases the charge distribution was significantly higher than that predicted by Boltzmann's distribution.

Key words: Respirable dust; Long-lived radioactive dust; electrical charge.

*Research Scientist and Radiation; Respirable Dust; Ventilation Project Leader, Elliot Lake Laboratory, CANMET, Energy, Mines and Resources Canada, Elliot Lake, Ontario, Canada. P5A 2J6.

INTRODUCTION

The short-lived decay products of ^{222}Rn and ^{220}Rn are formed initially in an atomic, positively charged state which rapidly combine with submicron aerosols (Porstendörfer and Mercer 1979; Dua et al. 1983; Szucs and Delfosse 1965; Wellisch 1913). As aerosols are found in positively, negatively and neutrally charged states, the resulting atmosphere consists of a complex mixture of charged and neutral particles of a size covering a wide range.

Field measurements have shown that industrial dusts in the respirable size range carry an electrical charge (Johnston et al. 1985; 1987). As can be anticipated, Long-Lived Radioactive Dust (LLRD), i.e., dust containing long-lived radioisotopes, can also be shown (this paper) to be electrically charged. Long-Lived Radioactive Dust is generated in the course of mining operations in uranium mines.

The charge associated with LLRD in the respirable size range is of interest from the health physics standpoint since it influences the deposition of these particles in the human respiratory system (Prodi and Mulroni 1985).

Because of the electrical charge associated with LLRD, these radioactive particles can be influenced by external electric and magnetic fields (Fuchs 1964; Jonassen 1983; Bigu 1985; Bigu and Grenier 1986) thereby providing a means to reduce radiation levels in working areas.

The electrical characteristics of radioactive and non-radioactive aerosols, and industrial dusts, have been investigated by several workers (Porstendöfer and Mercer 1979; Johnston et al. 1985; Johnston et al 1987; Bigu 1985; Bigu and Grenier 1986; Billard and Madelaine 1967; Bricard et al.; Dua et al. 1978; Dua and Kotrappa 1981). This paper deals with the electrical characteristics of Long-Lived Radioactive Dust generated in the course of several mining operations in an underground uranium mine. This work

was carried out at a rock crusher and along a conveyor belt in an underground uranium mine.

An electrical elutriator of the two split-flow type was used in conjunction with a variety of radioactivity, aerosol and respirable dust measuring instrumentation.

DESCRIPTION OF THE APPARATUS

The electrical elutriator, heretofore commonly referred to as the Split-Flow Elutriator (SFE), was originally designed by Johnston (1983) and duplicated at the Elliot Lake Laboratory (Grenier and Butler 1988).

The SFE basically consists of two halves that make up the main body of the elutriator, a flow-splitting end cap and two stainless steel parallel plates to which a variable voltage can be applied. The main body and the flow-splitting assembly are made from high-resistivity laminated epoxy resin sheets.

The elutriator channel, lined with the steel plates, is 35 cm in length, 8.6 cm in width, and 0.8 cm in height.

The size of the SFE channel was designed to operate at a nominal flowrate of 3 L min^{-1}. This flowrate permits laminar flow conditions in the channel and provides an air clearance time of less than 5 sec.

The particular design of the flow-splitting assembly allows the SFE to be used under two different modes of operation of practical interest (Johnston 1983), namely:

1. Determination of the charge distribution of the dust cloud without polarity discrimination: heretofore referred to as configuration X;
2. Determination of dust cloud charge distribution with polarity discrimination, i.e., both polarities are simultaneously measured, heretofore referred to as configuration Y.

In the first case (configuration X), all sampling ports in the flow-splitting assembly are connected together and counted by means of, say, an optical particle counter.

In the second case (configuration Y), the sampling ports in the flow-splitting assembly of the SFE are connected to two different dust concentration monitors, or any similar arrangement for some specific purpose other than that described in this paper.

In configuration X (top Fig. 1), the two SFE sampling ports were connected together and then fed to an optical particle counter (OPC)[+]. This particle counter can determine dust concentration in six different particle size ranges simultaneously, namely 0.5 to 1.5 μm; 1.5 to 2.0 μm; 2.0 to 3.5 μm; 3.5 to 5.0 μm; 5.0 to 10.0 μm; >10.0 μm.

In configuration Y (bottom Fig. 1), the two sampling sites of the SFE were run independently at 3 L min^{-1} each by means of two identical OPCs. Alternatively, one sampling site of the SFE could be fed to an OPC whereas the other sampling site could be connected to a sample holder to filter arrangement or cascade impactor for radioactivity measurement purposes.

It should be noted that configuration Y can also be realized by using one sampling site of the SFE in the manner described above while maintaining the other side at the same airflow by means of an external pump. Charge distribution information can be obtained by alternately reversing the polarity of the voltage applied to the plates of the SFE or by running a series of measurements with one polarity first, and then reversing the polarity.

Configuration Y was used to investigate the electrical characteristics of LLRD and LLRD exposed to a negative ion-generator. The ion-generator (IG) provided a means to deposit an electrical charge on dust.

[+]Modified HIAC/ROYCO Model 4100, manufactured by Mono Research Laboratories Limited, 300 Hwy 7W, Brampton, ON, Canada.

Measurements with the SFE were made by varying the external DC voltage applied to the SFE plates between 0 and $\pm$ 5000 V. The DC voltage was provided by an external DC power supply.

THEORETICAL BACKGROUND

It can be shown that the number of elementary charges, n, on a particle under field charging conditions is given by (Johnston 1983; Hochrainer 1985):

$$n = \frac{3\pi\mu\eta\ D_p}{eC} \qquad (1)$$

where, η is the air viscosity

D_p is the particle diameter

μ is the particle mobility

e is the electron charge

C is the Cunningham slip correction (~1)

The mobility of the particle can be obtained from the flowrate conditions and the physical dimensions of the SFE as follows (Johnston 1983; Hochrainer 1985):

$$\mu = F(\frac{Q}{V_o}) \qquad (2)$$

where, Q is the sampling flowrate ($m^3\ s^{-1}$)

F is a geometrical factor given by b:wl, where b, w and l are the physical dimensions of the SFE (i.e., w and l, are, respectively, the channel width and the channel length, whereas b is half the SFE channel height. All dimensions in m).

V_o is a voltage defined as follows: particle concentration data are tabulated as a function of voltage differential applied to the SFE. The data are then normalized to zero volt concentration and plotted. A tangent passing through the 50% normalized concentration point defines the voltage V_o by drawing a vertical line to the x-axis

(i.e., voltage) from tangent contact point (see Fig. 6).

Substituting eqn. (2) into eqn. (1), one gets the number of elementary charges on a particle of size D_p:

$$n = 3\pi FK\left(\frac{D_p}{V_o}\right) \tag{3}$$

where,

$$K = \frac{\eta Q}{eC} \tag{4}$$

Taking into account that for the SFE used here, w = 8.6 x 10^{-2} m, 1 = 0.35 m, and b = 4 x 10^{-3} m, it can be shown that eqn. 3 reduces to:

$$n = 7.036 \times 10^{9}\left(\frac{D_p}{V_o}\right) \tag{5}$$

where D_p is in meters.

The procedure outlined above (Johnston 1983) can be applied to particles of different sizes in a dust cloud in order to obtain the electrical charge distribution of the cloud. This procedure is straightforward for clouds with symmetric charge distributions, i.e., number of positively charged particles equals number of negatively charged particles. For clouds with asymmetric charge distributions, however, the procedure is more complex as described by Johnston elsewhere (Johnston 1983).

Aerosols in the submicron range and airborne dust in the respirable size range interact with bipolar and unipolar atmospheres in a rather complex way. For radioactive and non-radioactive aerosols and dust found in an electrically charged state in underground uranium mines, the following competing mechanisms of interaction are operative: diffusion charging (Gunn 1954); electrical neutralization (Liu and Pui 1974); electrical self-charging effects (Yeh 1976); α-particle recoil (Fleischer 1980; 1983); and electron charge transfer. It should be noted that the electrical charge of dust depends on its production method. Piezoelectric, triboelectric, and possibly, exoelectron effects are believed to be responsible for the electrical charge

developed in dust produced during rock crushing operations. Friction, collisions, bouncing, and rock shaking are believed to play an important role in the production of dust during transportation operations.

Charge neutralization occurs because of ion-pairs produced by ionization of mine air by ^{222}Rn (and ^{220}Rn) progeny. Self-charging effects are caused by radionuclides contained in aerosols and dust particles. Diffusion charging arises from attachment or adsorption of ions from ion-pairs produced in mine air by ^{222}Rn and ^{220}Rn progenies. Alpha-recoil arises from α-particle emission by some long-lived radioactive dust nuclides, ^{222}Rn, ^{220}Rn, and some of their short-lived decay products. Electron charge transfer is brought about by transfer of free electrons from one molecular species or ions to another.

The above processes are further complicated in uranium mines because respirable dust contains, in addition to long-lived radionuclides such as ^{228}U, ^{232}Th and ^{226}Ra, the following:

a) Short-lived decay products of ^{222}Rn and ^{220}Rn formed by the radioactive decay of U and Th radioisotopes. These products are continuously being formed because of the presence of their long-lived parents;

b) Short-lived decay products of ^{222}Rn and ^{220}Rn attached to the surface of airborne particles.

Items a) and b) are not only important in connection with self-charging effects, but they also affect neutralization and diffusion charging mechanisms.

Neutralization of charged aerosols in a bipolar atmosphere has been investigated theoretically and experimentally by Liu and Pui (1974). Their work has been extended by Yeh (1976), who considered neutralization of self-charging aerosols (e.g., radioactive particles). Diffusion charging has been studied by Gunn (1954).

EXPERIMENTAL PROCEDURE AND FURTHER COMMENTS

The split-flow elutriator (SFE) was used in configurations X and Y in an underground uranium mine to investigate the electrical characteristics of LLRD near a rock breaking operation (crusher), and an uranium ore transportation system (conveyor belt).

Dust and LLRD concentration and size distribution measurements were conducted using an eight-stage cascade impactor[±] operated at a flowrate of 10 L min^{-1}. This instrument also provided Mass Median Aerodynamic Diameter (MMAD) and Activity Median Aerodynamic Diameter (AMAD) data. In addition, LLRD gross α-particle activity was measured on the substrates of the cascade impactor using conventional instrumentation. Independent, but concurrent, measurements of dust mass were also made by means of a continuous dust monitor[6]. Furthermore, and in conjunction with SFE measurements, dust concentration and size distribution were determined using six-size range optical particle counters (OPC)[″], see below.

Rn-222 progeny and ^{220}Rn progeny concentration measurements were carried out using the Thomas-Tsivoglou (1972) and Rock (1975) methods, respectively. These data were subsequently used to calculate ion-pair production rates, ion-pair concentration and progeny attachment rates to LLRD (Bigu 1988).

The experimental apparatus shown in Fig. 1 permits the determination of an 'average' electrical charge associated with the radioactive dust cloud. This is accomplished by measuring the LLRD α-particle activity deposited on a

---

[±]Model 210, distributed by Andersen, 4215 Wendell Drive, Atlanta GA 30336.
[6]Model Mini-Ram PDM-3, manufactured by GCA Corporation, Technology Division, 213 Burlington Road, Bedford, Mass 01730.
[″]Modified HIAC/ROYCO Model 4100, manufactured by Mono Research Laboratories Limited, 300 Hwy 7W, Brampton, ON, Canada.

series of samples (i.e., filters) taken at different electrical voltages on the SFE and using Johnston's method, as described above. However, unless the particle size range of the dust cloud is very narrow, i.e., preferably ~1 μm, a few μm at most, the value obtained for the electrical charge provides only limited information and its practical usefulness, is therefore, severely curtailed.

If detailed information is sought on the electrical charge (n) associated with a given radioactive dust particle size (D_p), and of the dust cloud spectral distribution (i.e., n versus D_p), then a means for particle size selection is required. Such means is provided by using a multi-stage cascade impactor covering the particle size range of interest, instead of the 'integral' sample holder to filter system.

There are essentially four different experimental arrangements that can be used to determine the electrical charge on LLRD. They all involve the measurement of LLRD α-particle activity on a series of samples or set of samples taken at different electrical voltages on the SFE. Two such arrangements can provide an 'average' electrical charge (n) for the entire dust cloud size range (items 1 and 2). The third arrangement can provide an average n for the respirable size range (item 3), whereas the fourth arrangement gives spectral information, i.e., n versus D_p, namely:

1. Use of simple in-line filter holder housing a conventional 'absolute' filter. Dust size concentration and size distribution can be obtained by concurrent measurements using the OPC;
2. Use of arrangement indicated in item 1, but substituting the conventional absolute filter (e.g., glass fibre) by silver membrane filter (5 μm pore diameter size) which permits dust quantification, as well as independent α-particle activity measurement, by X-ray diffraction analysis;
3. Substitute in-line filter holder in items 1 and 2 by respirable dust

sampler of say, the cyclone type. This arrangement collects dust in the respirable size range (~1 to 10 μm) as opposed to total dust (i.e., <1 μm to >10 μm) as in items 1 and 2;

4. Substitute simple in-line sample holder to filter system or respirable dust sampler (i.e., respirable dust size selector) by, say, a multi-stage cascade impactor.

Field measurements of the type described above are extremely difficult to conduct in underground uranium mines and uranium mills during mining and milling operations for the following reasons:

1. Unless the long-lived radionuclide (e.g., ^{238}U, ^{232}Th, ^{224}Ra and ^{226}Ra) content in dust particles is rather high, the α-particle activity on the samples is quite low. Hence, long sampling times for each electrical voltage setting on the SFE are necessary;
2. Particle size distribution and dust concentration levels during mining and milling operations are highly variable and, hence, do not remain reasonably constant for more than a few minutes at best. This time is much shorter than that required for sampling purposes and for good, or reasonably acceptable, LLRD α-particle counting statistics;
3. Rn-222 and ^{220}Rn progeny concentrations during mining and milling operations do not remain constant and can easily vary by a factor of two or more depending on ventilation conditions, mining operation schedules, aerosol concentration fron dieselized equipment, and other factors. Rn-222 and ^{220}Rn progeny concentrations are important because they determine ion-pair production and the magnitude of attachment of these progenies to LLRD. Both mechanisms can greatly affect electrical neutralization and electrical charging processes in LLRD, as previously discussed;
4. The sampling flowrate of the SFE is about 3 L min^{-1} providing a transit

time for dust of ~5 s. Although optimum for the performance of the SFE, this flowrate is not quite adequate for sampling LLRD.

For the reasons outlined above, these particular types of measurements are more readily conducted in the laboratory where strictly controlled conditions can reasonably be maintained. Hence, because of the experimental difficulties encountered under field conditions, LLRD α-particle activity measurements with the SFE were not conducted. Instead, an OPC (apparatus which does not distinguish between radioactive and non-radioactive dust) was used in the manner previously indicated, and concurrent, independent, measurements of LLRD concentration and size distribution were made during electrical charge measurements with the SFE. (The reader should be aware that because of self-charging effects arising from the long-lived radionuclides content of the dust, and the interaction of this charge with airborne electrically charged particles, the electrical charge characteristics of LLRD should not be expected to be the same as that of the same dust but devoid of these radionuclides.)

EXPERIMENTAL RESULTS

Figures 2 and 3 show dust concentration measurements, versus time, in three dust particle size ranges, namely, 0.5 to 1.5 μm, 2.0 to 3.5 μm, and 5 to 10 μm conducted at the conveyor belt (Fig. 2) and the crusher platform (Fig. 3). (Other size ranges have been omitted for simplicity and because of space limitations. The air temperature and relative humidity were, respectively, 14^{o}C and 85%.) Although numerous electrical charge measurements were conducted, the data presented here are related to Figs. 2 and 3. These data were taken with one of the two Optical Particle Counters (OPC's) which was used as a dust monitoring device, whereas the other was used in configuration X (see Fig. 1) for electrical charge measurements.

Figures 2 and 3 show the great variability in dust concentration over relatively short periods of time at the experimental locations. (This variability depends on whether the crusher and or conveyor belt are operating and whether rock is being crushed and or transported.) They also show large differences in particle size distribution within the several size ranges investigated. By number, over 65 to 85% (depending on the mining operation, i.e., ore transportation or rock crushing) of the particles in the dust cloud were in the range 0.5 to 1.5 μm. Dust concentrations in the 1.5 to 2 μm and 2 to 3.5 μm were similar, although the concentration corresponding to the smaller particle size range was significantly higher than that corresponding to the range 2 to 3.5 μm. Few particles were of size larger than 10 μm as compared with smaller size particles. During full operation of the crusher or the conveyor belt, the total dust particle concentration was ~2 x 10^5 cm^{-3}. In terms of mass, a dust concentration of ~0.065 mg m^{-3} was obtained using the Mini-Ram PDM-3 continuous dust monitor.

Further analysis of the data shows a wide range of values for the time taken for the dust concentration to reach a steady-state (i.e., ~6 to >30 min) depending on ventilation conditions, the mining operation, and dust concentration growth modality, i.e., build-up (operation off > on) or decay (operation on > off).

The electrical charge measurements on dust particles reported here were conducted during mining activity periods as near to steady-state as practically possible. Other data obtained under less favourable conditions, i.e., strong variability, were used for analysis where dynamic situations are of interest. Measurements under 'quasi steady-state conditions', such as the ones reported here, lasted, on average, about 5 min for a complete run.

Figure 4 shows the percentage cumulative α-particle activity (LLRD) and dust mass (Total Dust) versus the Equivalent Aerodynamic Diameter EAD($D_{P,50}$)

obtained from measurements of the cascade impactor substrates. Also shown in the Fig. is the percentage cumulative α-particle activity (LLRD) versus EAD($D_{P,50}$) for the ^{220}Rn progeny collected on the substrates during the same sampling period. (Because of the short-lived activity of the ^{222}Rn progeny, a graph similar to that of the ^{220}Rn progeny count could not be obtained.)

From the graphs in Fig. 4, the Mass Median Aerodynamic Diameter (MMAD) and Activity Median Aerodynamic Diameter (AMAD) for the long-lived radioactive dust could be estimated as well as the AMAD for the ^{220}Rn progeny. The following values were obtained for this particular experiment: AMAD (LLRD) = 3 μm, AMAD (^{220}Rn progeny) = 0.3 μm, and MMAD = 2 μm. However, the following ranges of values were obtained from the above and several other experiments.

AMAD (LLRD) = 3.0 to 6.0 μm

AMAD (^{220}Rn progeny) = 0.2 to 0.3 μm

MMAD = 2.0 to 3.4 μm

Figure 5 shows the percentage of the total α-particle activity (LLRD) and dust mass (Total Dust) versus impactor stage cut-off size for the two mining operations monitored, namely, ore crushing (top illustration) and ore transportation (bottom illustration). The graphs shown in this Fig. indicate in a somewhat clearer fashion than in Fig. 4, that maximum mass and maximum α-particle activity (LLRD) occur in the approximate size range 2 to 3 μm. The data presented in Fig. 5 represent the average of two complete daily shifts (~8 h, i.e., 16 h total) in each case. (Note: there are insufficient data to ascribe any particular meaning or difference to these somewhat different particle size distributions from cascade impactor data for the limited period of underground experimentation, i.e., 2d at the crusher and 3d at the conveyor belt.)

Figure 6 shows the normalized dust concentration versus electrical

voltage on the SFE for two particle size ranges, namely, 0.5 to 1.5 μm and 3.5 to 5.0 μm. These data were taken at the crusher platform and illustrate Johnston's (1983) procedure to obtain V_o (see eqn (5)). Once V_o has been obtained substitution into eqn. (5) gives the number of elementary electrical charges, n, on particles of size D_p. Figure 6 and eqn. (5) show that, as theoretically predicted, n increases with increasing particle size (D_p).

Figure 7 shows the electrical charge of dust versus particle size using configuration X for the two mining operations of interest, namely, crushing and ore transportation (conveyor belt). The data of Fig. 7 were obtained following the method illustrated in Fig. 5. These data can be represented by the analytical function:

$$n = K\, D_p^{\,m} \qquad (6)$$

where, K and m are numerical coefficients. Analysis of the data of Fig. 7 gives the following values for this coefficient: K = 1.91 and m = 1.55 for the conveyor belt, and K = 2.1 and m = 2.83 for the crushing operation. (It should be noted that the D_p values plotted in Fig. 7 correspond to the middle points of each particle size range of the OPC. Hence, the lines drawn in Fig. 7 do not necessarily represent the best fitting curves.)

Figure 7 shows a substantial difference in the electrical charge of dust for a given D_p for the two mining operations, namely, during the crushing operation, the value of n near the crusher was significantly higher than at the conveyor belt. The differences observed depend partly on the method of dust generation, and as previously indicated, on self-charging effects, charge neutralization, ionic charge acquisition, α-particle recoil mechanisms and electron charge transfer. The overall (net) effect of the dust production method, and charging and neutralization mechanisms on the production of electrical charge in dust particles is a function of the dust cloud residence time, where residence time is understood to be the time elapsed between the

production of the dust cloud and its measurement. The dust cloud residence time depends on the pathway(s) followed by the cloud.

For the dust size range investigated here (0.5 μm to $\lesssim$ 10 μm), the electrical charge varied from n = 1.8 (D_p = 1 μm) to n = 50 (D_p = 8 μm) for the ore transportation operation, and from n ~3.5 (D_p = 1 μm), to $\lesssim$ 500 (D_p = 8 μm) for the rock crushing operation. For a MMAD and AMAD of ~3 μm, typical of the mining operations investigated here, the electrical charge on dust was n ~11 for the conveyor belt, and n = 55 for the rock crushing operation.

Table 1 shows ^{222}Rn progeny and ^{220}Rn progeny data (daily averages) taken at the crusher platform and the conveyor belt during the one week of experimentation. The electrical charge data of Fig. 7 were obtained on the days marked with an asterisk. Radiation conditions within a given day (working shift) remained reasonably constant. However, a variation of up to a factor of 2 was observed between different days. Other data of interest are given below:

a) Specific long-lived α-particle activity of dust (average): 500 mBq mg^{-1};

b) Long-lived radioactive dust concentration (α-particle activity): 30-41 mBq m^{-3};

c) ~95% of ^{222}Rn progeny and ^{220}Rn progeny activity was found associated with particles of size well below 1 μm.

DISCUSSION

Because the distance between the crusher jaws and the sampling station, located at the crusher platform, was much shorter (~12 m) than the distance from the crusher conveyor belt transfer point to the sampling station at the conveyor belt (~100 m), it is tempting to attribute the differences observed in electrical charge on the dust cloud for these two mining operations to

mainly charge neutralization neglecting radioactivity self-charging, other potentially important effects, and the dust production method. (The different distances of the sampling stations to the experimental sites of interest were a practical constraint because of safety considerations.)

A rough estimate of the neutralization time, say t, can be obtained using Gunn's expression (1954):

$$t = \frac{1}{4\pi N e \mu} \tag{7}$$

The ion-pair (ip) concentration (N) in the mine atmosphere can be calculated from the ^{222}Rn progeny and ^{220}Rn progeny concentrations. Taking $N \sim 10^{10}$ ip m^{-3} (Bigu 1988), and assuming $D_p \sim 0.001$ μm with a mobility $\mu \sim 6 \times 10^{-2}$ m^2 (stat V)$^{-1}$ s^{-1}, the neutralization time can be calculated using eqn. 7. The result is $t \sim 0.28$ s.

A similar calculation can be made considering the neutralizing effect of the ^{222}Rn progeny and or ^{220}Rn progeny. Two cases are of interest, namely: the unattached fraction and the attached fraction. Using Yeh's formulation (Yeh 1976), the ratio of the final electrical charge, n_f, to the initial charge, n_i, on a self-charging particle of self-charging rate, S, can be calculated (Bigu 1988). The results of this calculation for the ion-pair case, and the unattached and attached progeny cases, for the crusher platform and the conveyor belt, are given in Table 2. The neutralization times for the crusher and the conveyor belt have been taken at 60 s and 300 s, respectively. These values represent the dust residence times, i.e., the time taken for the dust cloud to travel from the crusher jaws to the crusher platform sampling station, and from the former to the conveyor belt sampling station. The above residence times have been estimated from dust concentration profile records versus time by observing the dust concentration growth and decay during operation and interruption of the crusher and conveyor belt, respectively.

The data shown in Table 2 and Fig. 7 indicate:

1. Attached ^{222}Rn progeny and ^{220}Rn progeny are not effective in electrical neutralization processes because of their relatively large size, and hence low mobility, necessitating considerably longer neutralization times than ion-pairs;
2. Unattached ^{222}Rn progeny and ^{220}Rn progeny are quite effective as 'neutralizing' particles but their concentration was orders of magnitudes lower than that of ion-pairs;
3. Neutralization effects from ion-pairs had long occurred for dust residence times much less than 60 s. Hence, the dust electrical charge distributions measured at the crusher platform and the conveyor belt should be expected to be similar, on residence time arguments alone;
4. The dust electrical charge distributions shown in Fig. 7 are well above the Boltzmann's distribution shown in the same graph.

The arguments above suggest that: i) part of the differences in charge distribution may be related to the different mechanisms of dust production; ii) electrical charging mechanisms should not be ignored. A relatively detailed discussion on charging mechanisms, and their quantitative role in the context of this paper has been given elsewhere (Bigu 1988a). The quantitative description referred to in this reference includes the following mechanisms. Neutralization effects; self-charging effects due to the presence of radionuclides in long-lived radioactive dust; diffusion-charging; charging effects arising from α-particle recoil mechanisms; and electron charge transfer. A preliminary investigation on the electrical charge characteristics of LLRD and ^{222}Rn progeny has been discussed elsewhere (Bigu 1988b).

Because the primary goal of the work undertaken here was to initiate a preliminary study on the electrical charge characteristics of long-lived

radioactive dust in underground U-mines and U-mills, the design of the experiments and the data derived from them are neither sufficient nor adequate for a satisfactory quantitative and qualitative understanding of electrical charge neutralization and electrical charging mechanisms and processes of radioactive dust in ^{222}Rn, ^{220}Rn progeny atmospheres. This is best done in the laboratory under controlled conditions. Experiments to that effect are at present in progress in order to shed light on the contribution to electrical particle charge by diffusion charging, electrical charge neutralization, electrical self-charging mechanisms, charging by α-recoil processes and, possibly, electron charge transfer effects. These experiments are conducted in a large Radon, Thoron Test Facility (RTTF) of the walk-in type and a specially designed dust tunnel which enable the injection of arbitrary mixtures of ^{222}Rn and ^{220}Rn within a wide concentration range, as well as controlled temperature, relative humidity, aerosol composition, concentration, and size distribution (Bigu 1984). Experiments are carried out with uranium tailings dust and uranium mine dust of several ore grades, i.e., radioisotopic composition and concentration. Furthermore, and in order to confirm the above field results and the current laboratory work, electrical charge data obtained with the SFE will be compared with measurements using more conventional (historically speaking) apparatuses such as electrical elutriators of the cylindrical type (e.g., Zeleny tubes), and of the parallel plate type. These investigations are expected to contribute greatly to a better understanding of the electrical charge characteristics of long-lived radioactive dust, and hence, to the health hazards associated with its inhalation in the work place.

CONCLUSIONS

The electrical charge characteristics of long-lived radioactive dust have been investigated for two uranium mine operations. The electrical charge

associated with dust generated in a primary crushing operation was substantially higher than that corresponding to the ore transportation by a conveyor belt. In both cases, the charge distribution was significantly higher than that predicted by Boltzmann's distribution.

REFERENCES

Bigu, J. A walk-in radon/thoron test facility. Am. Ind. Hyg. Assoc. J. 45:525-532; 1984.

Bigu, J. Effects of electrical fields on ^{220}Rn progeny concentration. Health Phys. 49:512-516; 1985.

Bigu, J.; Grenier, M.G. Electrical characteristics of the short-lived decay products of thoron in underground uranium mines. Am. Ind. Hyg. Assoc. J. 47:308-311; 1986.

Bigu, J. Electrical charge characteristics of long-lived radioactive dust in underground uranium mine operations. Elliot Lake Laboratory, CANMET (EMR), Elliot Lake, ON; Division Report MRL 88-143(TR); 1988a.

Bigu, J. An instrument to determine the electrical characteristics of radioactive aerosol and long-lived radioactive dust. In: Proceedings of the 22nd Midyear Meeting of the Health Physics Society, San Antonio, Texas; 1988b:446-455.

Billard, F.; Madelaine, G. Study of electrical charge of aerosols. In Assessment of Airborne Radioactivity. Proc. of a Symposium held by the International Atomic Energy Agency (IAEA), Vienna; EAEA-SM-95/13: 325-333; 1967.

Bricard, J.; Renoux, A.; Pradel, J; Madelaine, G. Spectrum of natural aerosols. In: La Pollution Radioactive des Milieux Gazeux; 15-17.

Dua, S.K.; Kotrappa, P.; Bhanti, D.P. Electrostatic charge on decay products of thoron. Am. Ind. Hyg. Assoc. J. 39:339-345; 1978.

Dua, S.K.; Kotrappa. P. Comment on the charge on decay products of thoron and radon. Am. Ind. Hyg. Assoc. J. 42:242-243; 1981.

Dua, S.K.; Kotrappa, P.; Gupta, P.C. Influence of relative humidity on the charged fraction of decay products of radon and thoron. Health Phys.

45:152-156; 1983.

Fleischer, R.L. Isotopic disequilibrium of uranium: alpha-recoil damage and preferential solution effects. Science 207:979-981; 1980.

Fleischer, R.L. Theory of alpha-recoil effects on radon release and isotopic disequilibrium. Geochimica et Cosmochimica Acta 47:779-784; 1983.

Fuchs, N.A. The Mechanics of Aerosols. The MacMillan Company, New York; 1964.

Grenier, M.G.; Butler, K. Evaluation of a split-flow elutriator used in the determination of airborne dust charge distributions. Elliot Lake Laboratory, CANMET (EMR), Elliot Lake, ON; Division Report MRL 87-187(TR); 1988.

Gunn, R. Diffusion charging of atmospheric droplets by ions, and the resulting combination coefficients. J. of Meteorology 11:339-347; 1954.

Hochrainer, D. Measurement methods for electric charges on aerosols. Ann. Occup. Hyg. Assoc. J. 29:241-249; 1985.

Johnston, A.M. A semi-automatic method for the assessment of electric charge carried by airborne dust. J. Aerosol Sci. 14:643-655; 1983.

Johnston, A.M.; Vincent, J.H.; Jones, A.D. Measurements of electric charge for workplace aerosols. Ann. Occup. Hyg. 29:271-284; 1985.

Johnston, A.M.; Vincent, J.H.; Jones, A.D. Electrical charge characteristics of dry aerosols produced by a number of laboratory mechanical dispensers. Aerosol Sci. and Tech. 6:115-127; 1987.

Jonassen, N. The effect of electric fields on ^{222}Rn daughter products in indoor air. Health Phys. 45:487-491; 1983.

Liu, B.Y.H.; Pui, D.Y.H. Electrical neutralization of aerosols. Aerosol Sci. 5:465-472; 1974.

Porstendörfer, J.; Mercer, T.T. Influence of electric charge and humidity upon the diffusion coefficient of radon decay products. Health Phys. 37:191-199; 1979.

Prodi, V.; Mularoni, A. Electrostatic lung deposition experiments with humans and animals. Ann. Occup. Hyg. 29:229-240; 1985.

Rock, R.L. Sampling mine atmospheres for potential alpha-energy due to the presence of radon-220 (thoron) daughters. Denver Technical Support Center; MESA Informational Report IR/1015; 1975.

Szucs, S.; Delfosse, J.M. Charge spectrum of recoiling ^{216}Po in the α-decay of ^{220}Rn. Phys. Rev. Letters 15:163-165; 1965.

Thomas, J.W. Measurement of radon daughters in air. Health Phys. 23:783-789; 1972.

Yeh, H. A theoretical study of electrical discharging of self-charging aerosols. J. Aerosol Sci. 7:343-349; 1976.

Wellisch, E.M. Philos. Mag. 26:623-635; 1913.

LIST OF ILLUSTRATIONS

operations: crushing (top), and ore transportation (conveyor belt, bottom).

Fig. 6. Normalized dust concentration at the crusher versus Split Flow Elutriator voltage for two dust size ranges: 0.5 to 1.5 μm and 3.5 to 5.0 μm.

Fig. 7. Electrical charge on dust particles versus particle size for two mining operations: crushing, and ore transportation (conveyor belt). Also shown is the Boltzmann's distribution (B.D.).

CONFIGURATION X

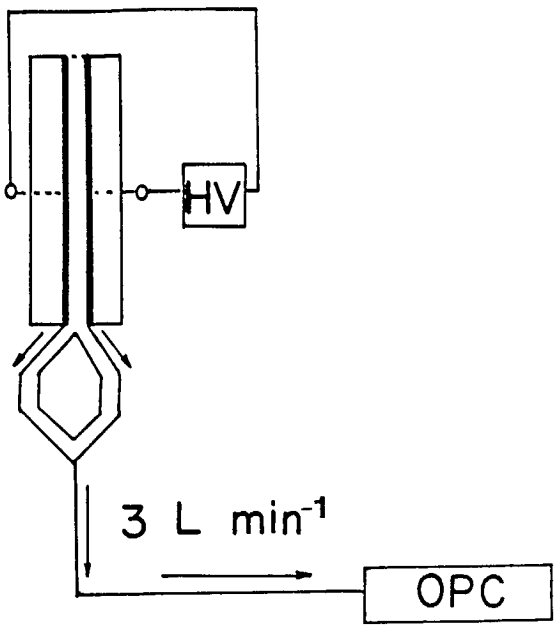

CONFIGURATION Y

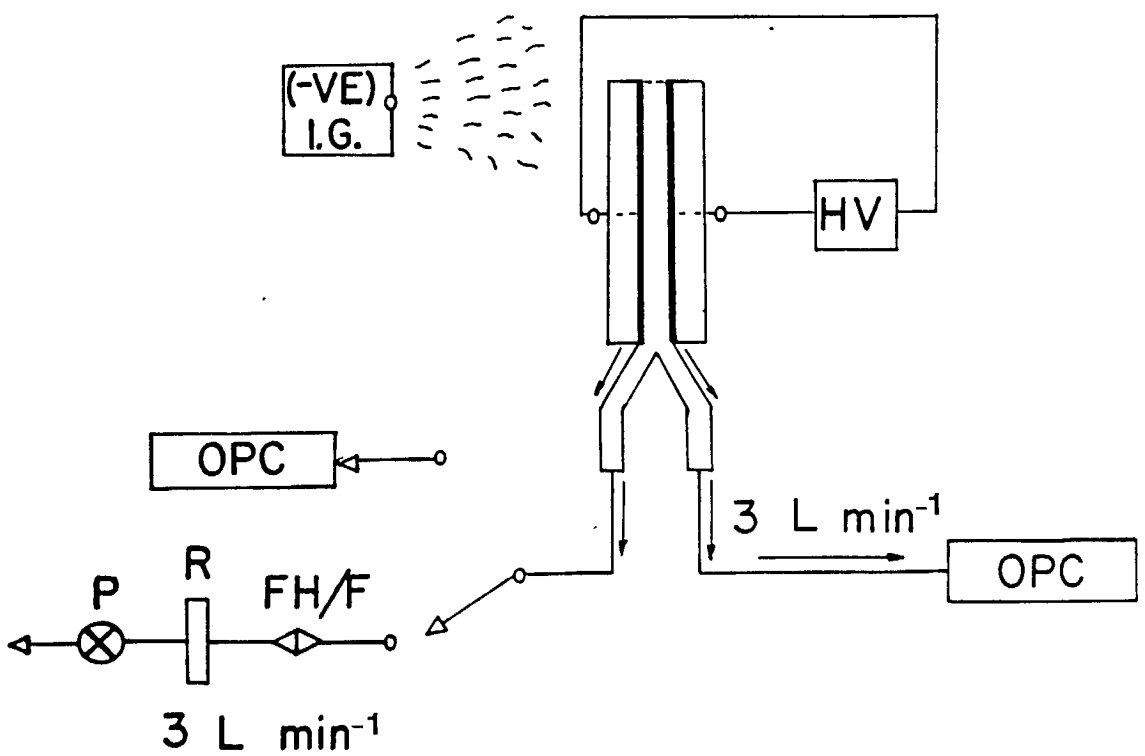

Figure 1

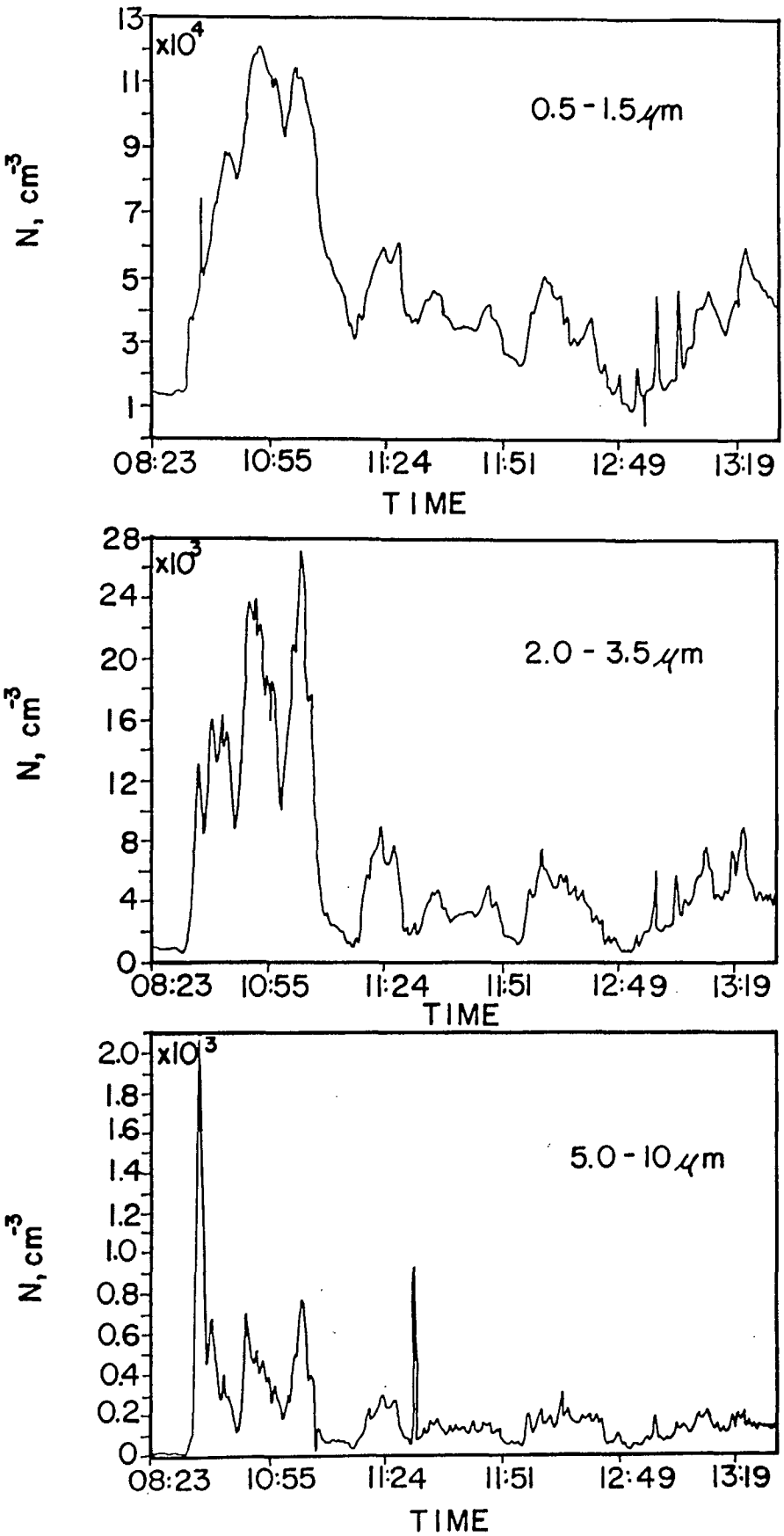
x10^4
0.5 - 1.5 μm
N, cm^-3
13
11
9
7
5
3
1
08:23
10:55
11:24
11:51
12:49
13:19
TIME
x10^3
2.0 - 3.5 μm
N, cm^-3
28
24
20
16
12
8
4
0
08:23
10:55
11:24
11:51
12:49
13:19
TIME
x10^3
5.0 - 10 μm
N, cm^-3
2.0
1.8
1.6
1.4
1.2
1.0
0.8
0.6
0.4
0.2
0
08:23
10:55
11:24
11:51
12:49
13:19
TIME

Figure 2

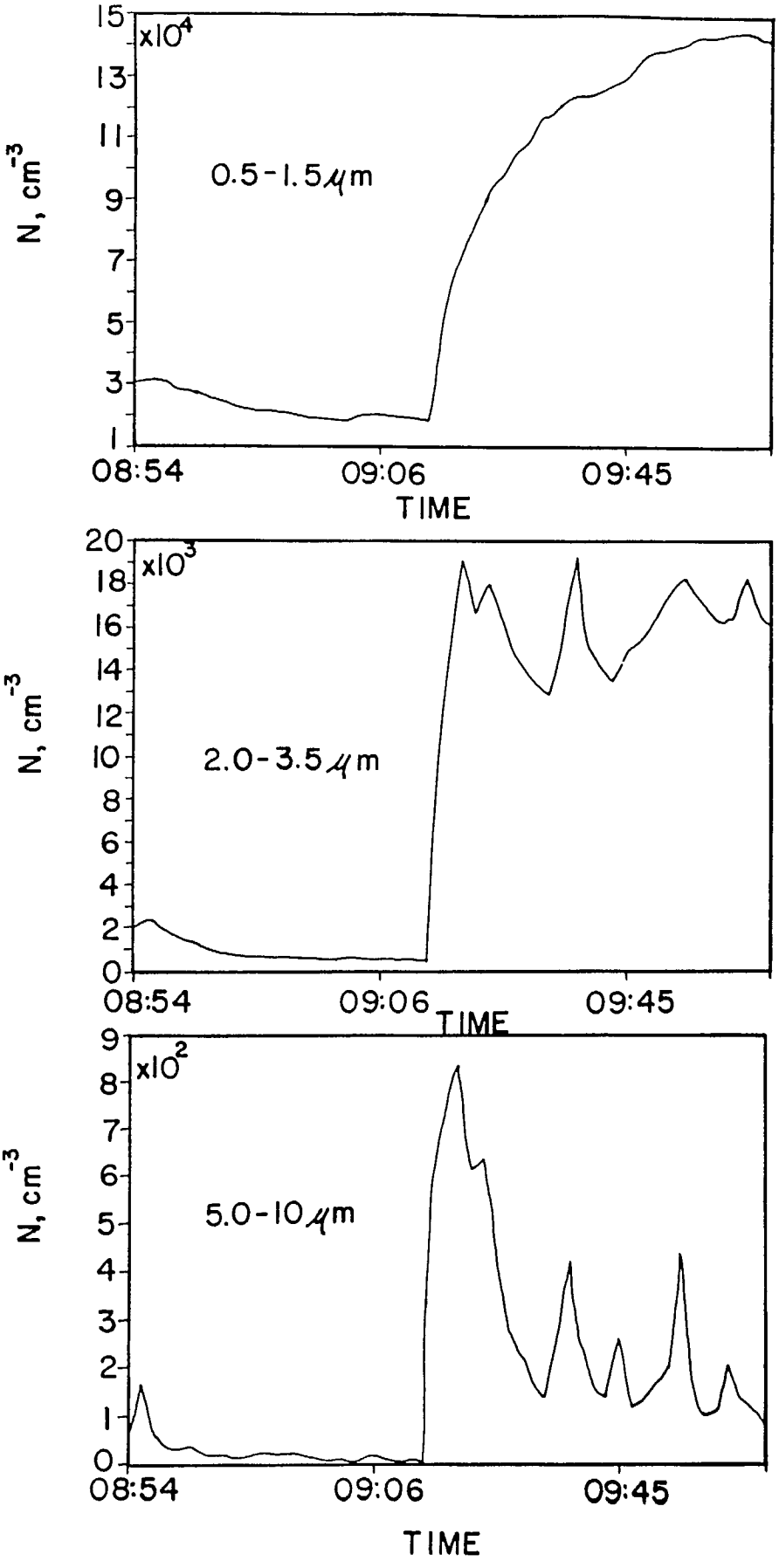
x10^4
0.5-1.5μm
N, cm^-3
15
13
11
9
7
5
3
1
08:54
09:06
09:45
TIME
x10^3
2.0-3.5μm
N, cm^-3
20
18
16
14
12
10
8
6
4
2
0
08:54
09:06
09:45
TIME
x10^2
5.0-10μm
N, cm^-3
9
8
7
6
5
4
3
2
1
0
08:54
09:06
09:45
TIME

Figure 3

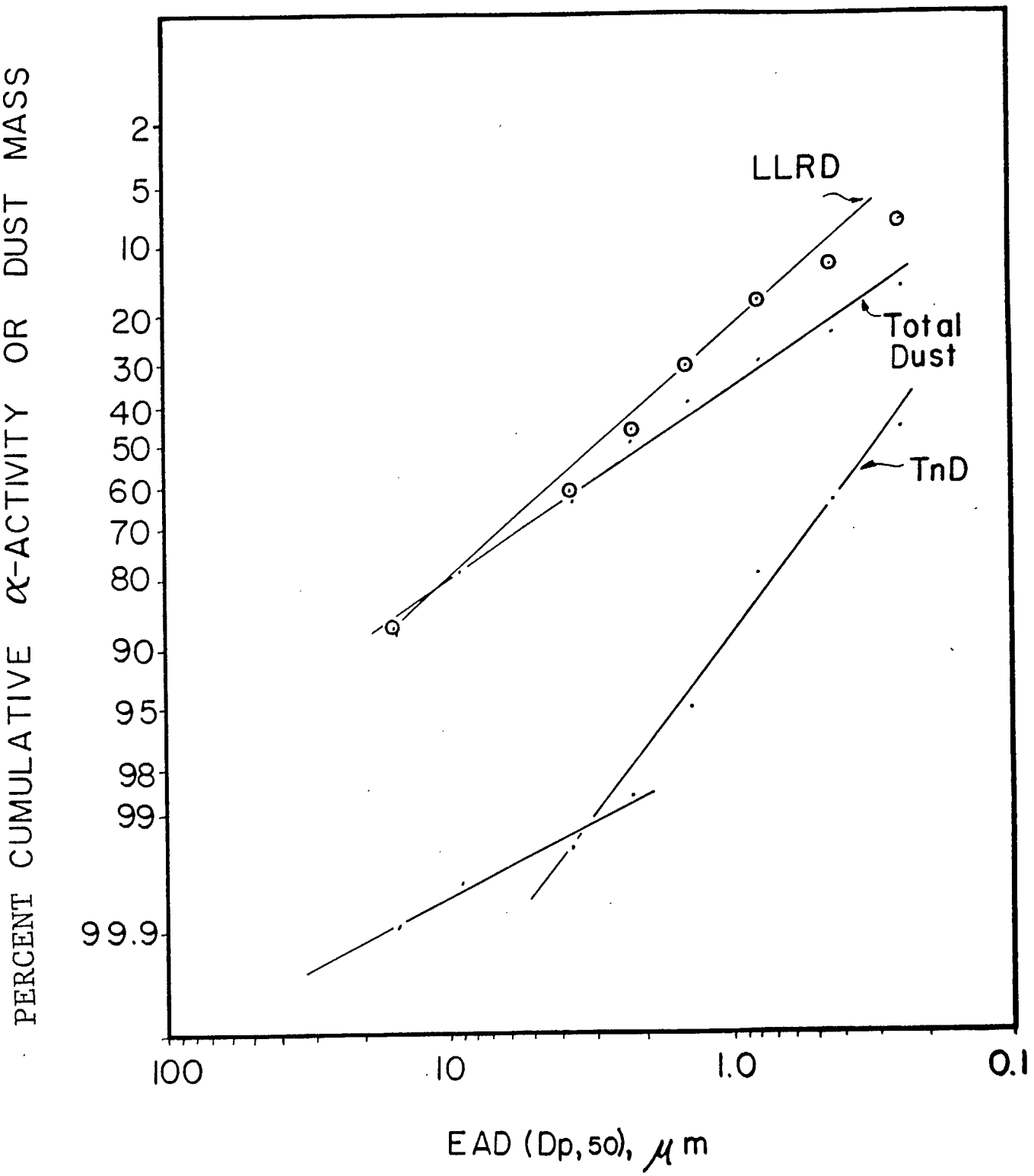
PERCENT CUMULATIVE α-ACTIVITY OR DUST MASS
2
5
10
20
30
40
50
60
70
80
90
95
98
99
99.9
LLRD
Total Dust
TnD
100
10
1.0
0.1
EAD (Dp, 50), μm

Figure 4

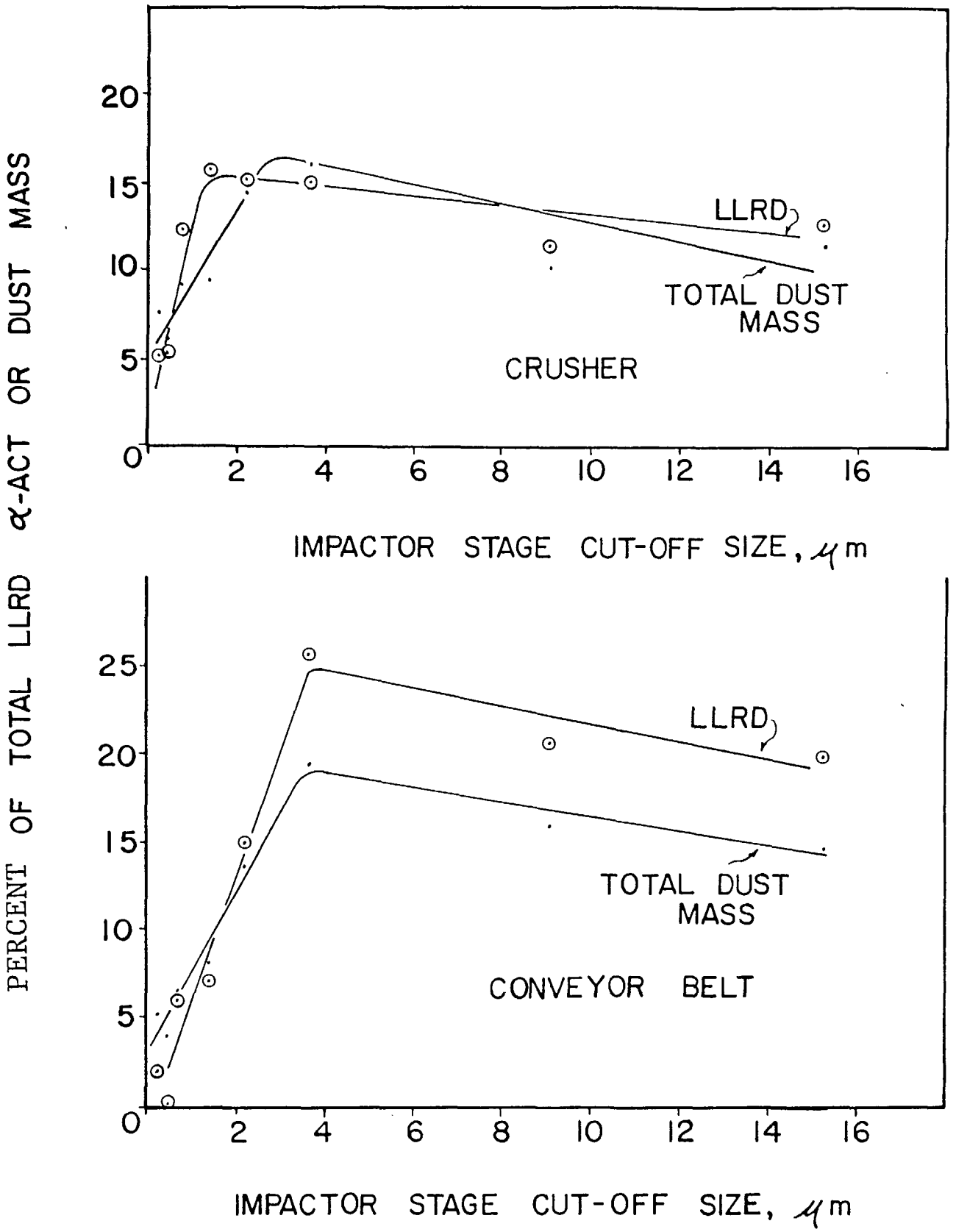
PERCENT OF TOTAL LLRD α-ACT OR DUST MASS
20
15
10
5
0
2
4
6
8
10
12
14
16
LLRD
TOTAL DUST MASS
CRUSHER
IMPACTOR STAGE CUT-OFF SIZE, μm
25
20
15
10
5
0
LLRD
TOTAL DUST MASS
CONVEYOR BELT
IMPACTOR STAGE CUT-OFF SIZE, μm

Figure 5

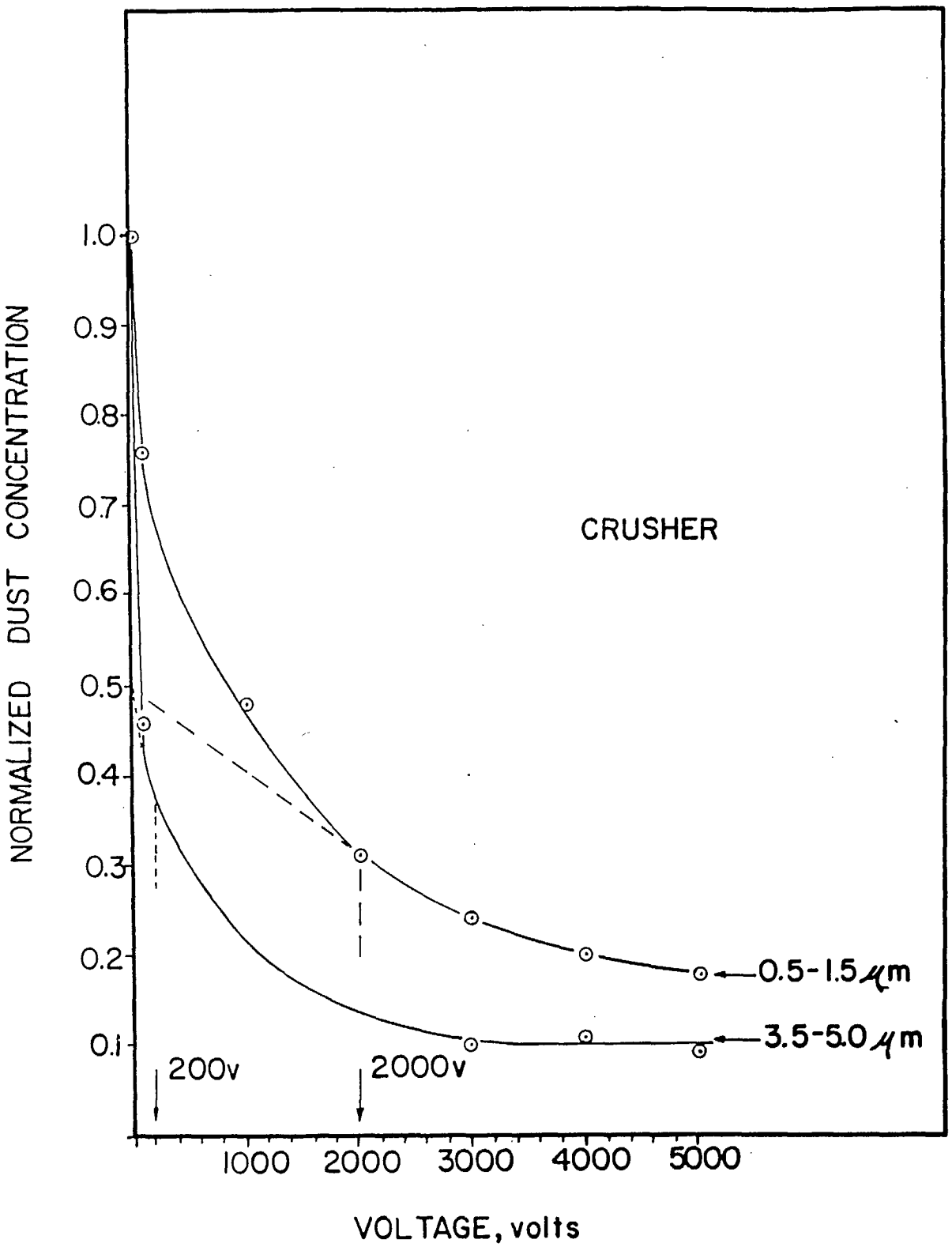
NORMALIZED DUST CONCENTRATION
1.0
0.9
0.8
0.7
0.6
0.5
0.4
0.3
0.2
0.1
CRUSHER
0.5-1.5 μm
3.5-5.0 μm
200v
2000v
1000
2000
3000
4000
5000
VOLTAGE, volts

Figure 6

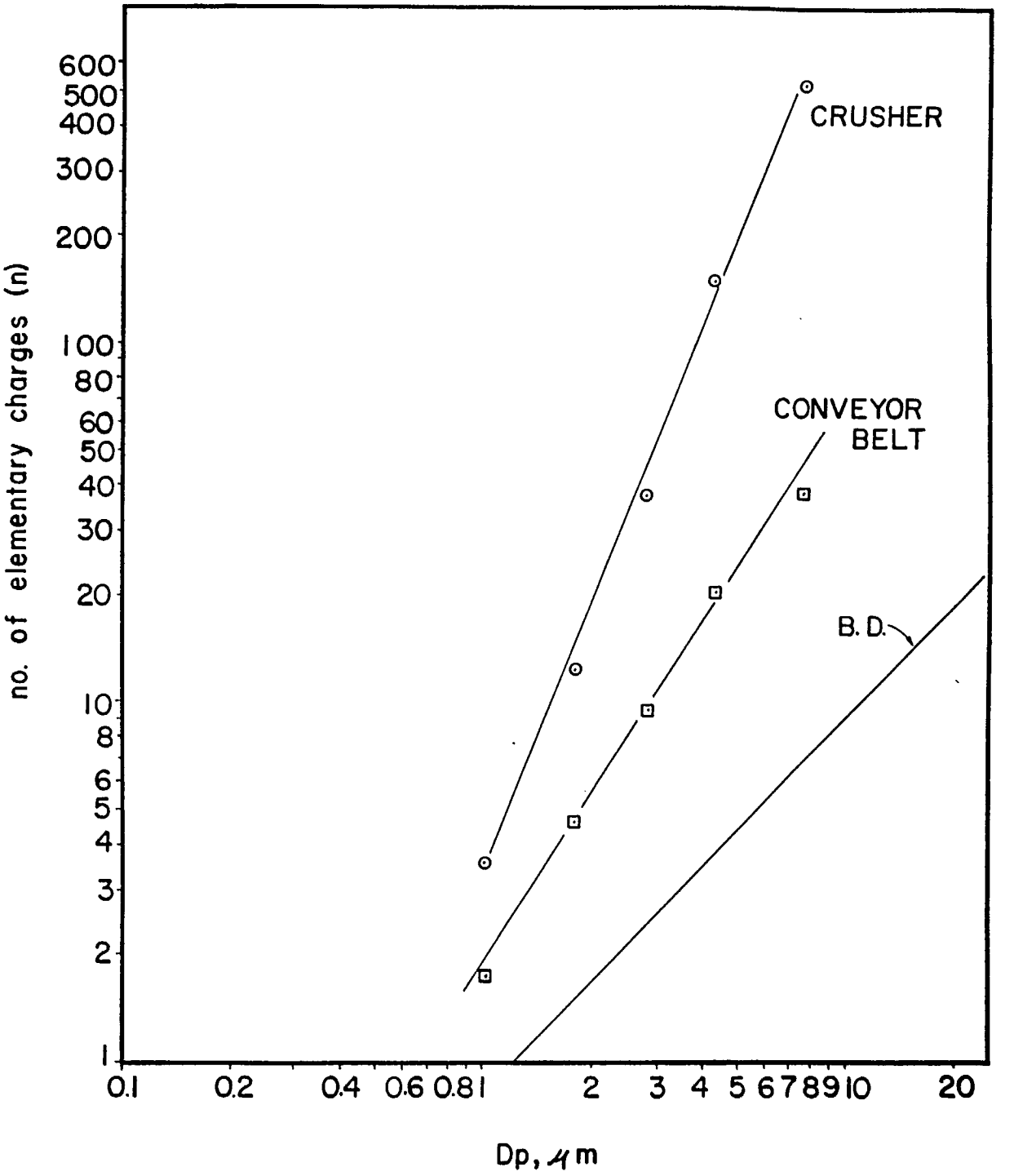
600
500
400
300
200
100
80
60
50
40
30
20
10
8
6
5
4
3
2
1
no. of elementary charges (n)
CRUSHER
CONVEYOR
BELT
B. D.
0.1
0.2
0.4
0.6
0.8
1
2
3
4
5
6
7
8
9
10
20
Dp, μm

Figure 7

LIST OF TABLES

Day	Working Location	$[^{218}Po]$ Bqm^{-3}	$[^{214}Pb]$ Bqm^{-3}	$[^{214}Bi]$ Bqm^{-3}	$[^{212}Pb]$ Bqm^{-3}	PAEC(Rn)[a] $\mu J\ m^{-3}$	PAEC(Tn)[a] $\mu J\ m^{-3}$
1	Crusher	1494	1154	962	70.2	6.19 (0.30)	4.78 (0.23)
2[b]	Crusher	1102	717	587	54.9	3.88 (0.19)	3.80 (0.18)
3	C.B.[c]	1346	845	510	51.9	4.27 (0.20)	3.61 (0.17)
4[b]	C.B.[c]	1014	612	450	42.7	3.28 (0.16)	2.86 (0.14)
5	C.B.[c]	1046	655	429	45.8	3.38 (0.16)	3.11 (0.15)

[a] The numbers in round brackets are given in Working Levels (WL). The conversion factor is 1 WL = 20.8 $\mu J\ m^{-3}$.

[b] The dates for which data are presented here.

[c] C.B. stands for conveyor belt.

Table 1

Case	t^a (s)	$n_f:n_i$ [b]	Remarks
Ion-pair	0.28	0 (0)	$N \sim 10^{10}$ ip m^{-3}; D_p = 0.001 μm; $\mu = 6 \times 10^{-2}$ m^2 (stat V)$^{-1}s^{-1}$
Unattached	2.76×10^3	0.98 (0.9)	$N(^{218}Po) \sim 10^6$ particles m^{-3}; D_p = 0.001 μm; $\mu = 6 \times 10^{-2}$ m^2 (stat V)$^{-1}s^{-1}$
Attached	1.8×10^7	1 (1)	$N(^{218}Po) \sim 10^6$ particles m^{-3}; D_p = 0.1 μm; $\mu = 9 \times 10^{-6}$ m^2 (stat V)$^{-1}s^{-1}$

[a] Neutralization time (t) calculated according to eqn. (7).

[b] Values on the left hand side and inside the round brackets refer to the crusher and conveyor belt, respectively.

Note: Calculations have been done for a LLRD α-particle activity of 500 mBq mg^{-1} (see text) which corresponds, approximately, to a self-charging rate: $S \sim 2 \times 10^{-8}$ Bq (particle)$^{-1}$ (Bigu 1988).

Table 2